

Article

# Theoretical Study of the Mechanism for CO<sub>2</sub> Hydrogenation to Methanol Catalyzed by *trans*-RuH<sub>2</sub>(CO)(dpa)

Jinxia Zhou <sup>1</sup>, Liangliang Huang <sup>2</sup>, Wei Yan <sup>1</sup>, Jun Li <sup>1,\*</sup>, Chang Liu <sup>1,\*</sup> and Xiaohua Lu <sup>1</sup>

<sup>1</sup> College of Chemical Engineering, Nanjing Tech University, Nanjing 210009, China; jaynazhou@163.com (J.Z.); xnrzyy@njtech.edu.cn (W.Y.); xhlu@njtech.edu.cn (X.L.)

<sup>2</sup> School of Chemical, Biological & Materials Engineering, University of Oklahoma, Norman, OK 73019, USA; HLL@ou.edu

\* Correspondence: lijun@njtech.edu.cn (J.L.); changliu@njtech.edu.cn (C.L.); Tel.: +86-159-0518-1806 (J.L.); +86-139-1393-9041 (C.L.)

Received: 6 May 2018; Accepted: 8 June 2018; Published: 11 June 2018



**Abstract:** In this work, the reaction mechanism for the conversion of CO<sub>2</sub> and H<sub>2</sub> to methanol has been researched by density functional theory (DFT). The production of methanol from CO<sub>2</sub> and H<sub>2</sub> is catalyzed by a univocal bifunctional pincer-type complex *trans*-RuH<sub>2</sub>(CO)(dpa) (dpa = bis-(2-diphenylphosphinoethyl)amine). The reaction mechanism includes three continuous catalytic processes: (1) CO<sub>2</sub> is converted to formic acid; (2) formic acid is converted to formaldehyde and water; (3) formaldehyde is converted to methanol. By computing the catalytic processes, we have shown that the rate-limiting step in the whole process is the direct cleavage of H<sub>2</sub>. The calculated largest free energy barrier is 21.6 kcal/mol. However, with the help of water, the free energy barrier can be lowered to 12.7 kcal/mol, which suggests viability of *trans*-RuH<sub>2</sub>(CO)(dpa) as a catalyst for the direct conversion of CO<sub>2</sub> and H<sub>2</sub> to methanol.

**Keywords:** CO<sub>2</sub> hydrogenation; formic acid; formaldehyde; methanol; *trans*-RuH<sub>2</sub>(CO)(dpa); density functional theory

## 1. Introduction

Methanol is a commonly used chemical [1,2], with annual production of around 70 million tons. It is commonly used to synthesize various chemical products. For example, methanol as a fuel is expected to alleviate the fossil energy crisis. Methanol can also be used as hydrogen storage material, as it contains 12.6 wt % hydrogen [3]. Commercially, methanol is generally synthesized from syngas using heterogeneous catalysts under high temperatures (200–300 °C) and pressures (5–10 MPa) [4]. The process requires that a certain amount of CO<sub>2</sub> be mixed with the syngas to improve the methanol production. Later, the synthesis of methanol from H<sub>2</sub> and CO<sub>2</sub> was studied. It is generally accepted that, due to the use of fossil fuels, the concentration of CO<sub>2</sub> has been increased by nearly 100 ppm since modern industrialization [5,6]. The increased atmospheric CO<sub>2</sub> is responsible for the global warming and other climate change related issues. The capture and sequestration of CO<sub>2</sub> [7,8] consumes lots of energy and resources. The conversion of CO<sub>2</sub> into commonly used chemicals and fuels [9–11] is an attractive strategy, which accords with sustainable development strategies. Methanol, as one of the main products [12–15] of CO<sub>2</sub> hydrogenation reactions, has attracted considerable research focus.

In recent years, CO<sub>2</sub> hydrogenation to methanol is the focus of much research in academia and industry. Generally, the process of CO<sub>2</sub> hydrogenation to methanol is conducted under heterogeneous [16] or homogeneous catalysts (see Table 1) [17]. Heterogeneous catalysts are mainly metals and metallic oxides, which have been used for catalytic carbon dioxide hydrogenation for

decades. However, for heterogeneous catalysts, hydrogenation reactions are mostly operated at relatively high pressures (>2.5 Mpa) and temperatures (>200 °C) [18–22]. The productivity and selectivity of methanol are limited, because the synthesis of methanol is an excessively exothermic reaction [23]. Compared with heterogeneous catalytic reactions, methanol may be synthesized from CO<sub>2</sub> with homogeneous catalysts at lower temperatures and pressures, thus increasing yield and selectivity. As for the recyclability and homogeneous catalyst separation from the reaction mixture, experiments have shown that the catalyst is supported on a relatively separated carrier, thus solving the problems. Loading the metal complex catalyst onto an easily separated carrier will hopefully solve the problem of homogeneous catalytic hydrogenation. Therefore, efficient homogeneous catalysts are preferred for CO<sub>2</sub> to methanol synthesis.

**Table 1.** The comparison of catalysts for CO<sub>2</sub> to methanol hydrogenation reaction.

	Heterogeneous Catalysts	Homogeneous Catalysts
Catalysts	Metal/Metallic oxide	Metal complex
Temperature	200–300 °C	Most are below 200 °C
Catalytic activity	Relatively low	Much higher than Heterogeneous

In 2011, Sanford reported the hydrogenation of CO<sub>2</sub> to CH<sub>3</sub>OH via three cascade catalysts [24]. However, in that catalytic reaction, only a low turnover number was achieved. Later on, Leitner and co-workers utilized a Ru-triphos (trimethylenemethane) complex for a CO<sub>2</sub> to methanol hydrogenation reaction [25]. The reaction mechanism of carbon dioxide reduction to methanol by Ru-triphos complex was investigated by Haunschild in 2015. In this research, the catalytic cycle can be split into three main sections [26]. However, the catalyst Ru-triphos contains air-sensitive phosphine ligands. Hence, the design of high-efficiency and phosphine-free metal catalysts used for the hydrogenation of CO<sub>2</sub> to CH<sub>3</sub>OH is highly desirable.

Recently, a bifunctional catalyst RuHCl(CO)(dpa) with polydentate chelating ligands bearing N-H functionalities (dpa = bis-(2-diphenylphosphinoethyl)amine) was synthesized by Kuriyama [27], and has been used for the catalytic hydrogenation of esters [28]. Since then, many selective hydrogenation reactions with RuHCl(CO)(dpa) have been reported. Subsequently, Ding et al. reported the RuHCl(CO)(dpa) catalytic hydrogenation of cyclic carbonates from readily-available CO<sub>2</sub> and epoxides, showing an excellent catalytic efficiency for methanol and corresponding diols [29]. Ikariya et al. reported the selective hydrogenation of fluorinated esters with RuHCl(CO)(dpa) or *trans*-RuH<sub>2</sub>(CO)(dpa) under mild conditions [30]. Their study demonstrates a good yield for fluorinated alcohols and hemiacetals. In addition, they also found that RuHCl(CO)(dpa) can be easily converted to the more effective catalyst *trans*-RuH<sub>2</sub>(CO)(dpa) with simple treatments.

Inspired by the aforementioned studies, in this work we seek a theoretical understanding of the hydrogenation reaction mechanism when using the catalyst *trans*-RuH<sub>2</sub>(CO)(dpa) for CO<sub>2</sub> to methanol conversion. As shown in Figure 1, the reaction mechanism includes three continuous catalytic processes.

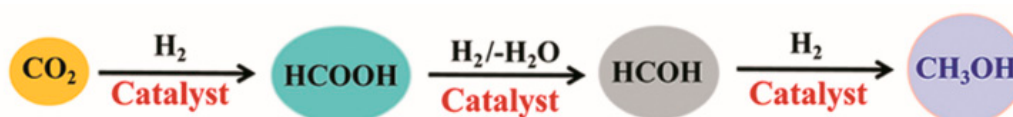
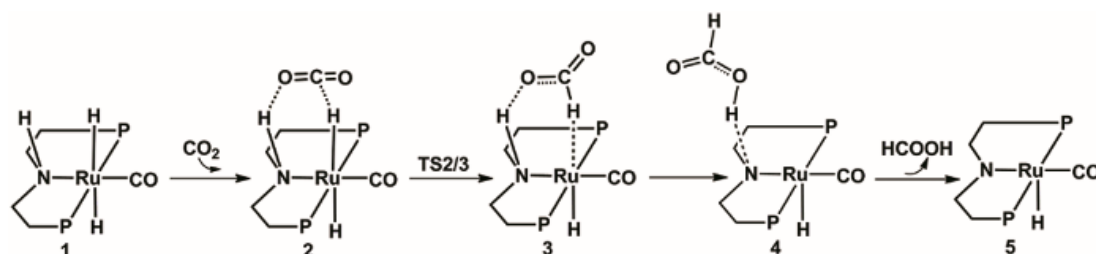


**Figure 1.** The three continuous catalytic processes of CO<sub>2</sub> hydrogenation to methanol.

## 2. Results and Discussion

### 2.1. Hydrogenation of Carbon Dioxide

The calculated catalytic process for the reduction of CO<sub>2</sub> to HCOOH is shown in Scheme 1. The free energy profile of the first catalytic process is shown in Figure 2. The optimized structures of transition state TS2/3 and key intermediate 4 are displayed in Figure 3.



**Scheme 1.** Predicted catalytic process for the hydrogenation of CO<sub>2</sub> to formic acid. Benzene on P atoms are omitted for clarity.

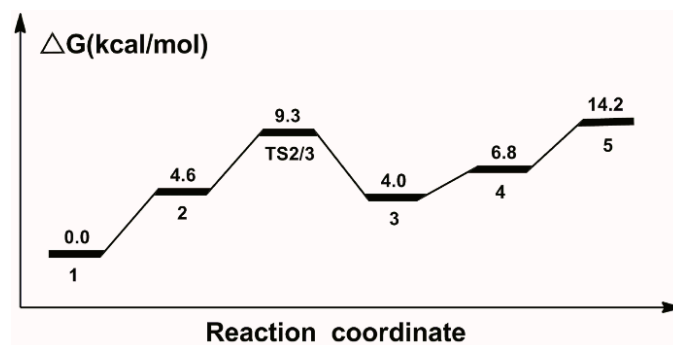


**Figure 2.** Calculated relative free energies in the catalytic process for the hydrogenation of CO<sub>2</sub> to formic acid.

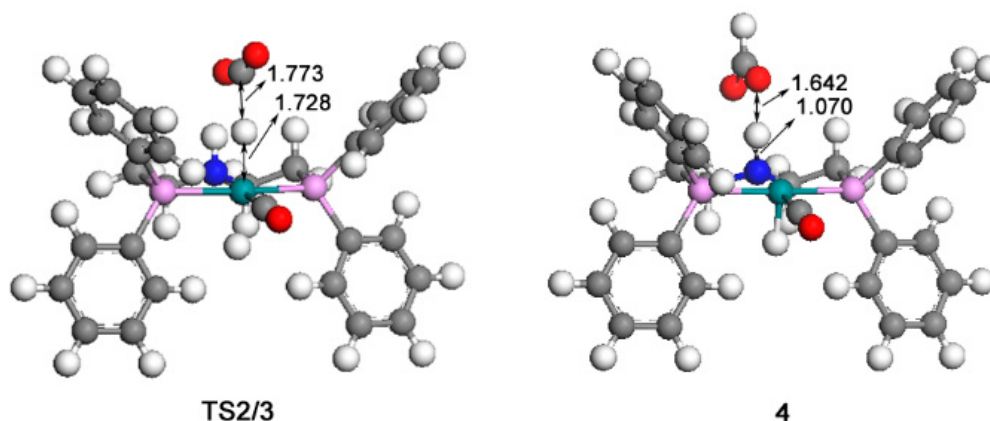


**Figure 3.** Optimized structures of TS2/3 (359i cm<sup>-1</sup>) and 4. The unit of bond lengths is expressed in angstrom (Å). (Green balls: Ru; pink: P; red: O; blue: N; grey: C; white: H).

The optimized structure of activated catalyst 1 (*trans*-RuH<sub>2</sub>(CO)(dpa)) (Figure 4) is a six-coordinated *trans*-dihydride ruthenium diphosphine complex bearing N-H functionalities with carbonyl ligands. The bond lengths of Ru-H1, Ru-H2, and N-H3 in catalyst 1 are 1.699 Å, 1.681 Å,

and 1.023 Å, respectively. The distances between the Ru and the two P atoms is, in both cases, 2.351 Å. The distance between the Ru and N atoms is 2.245 Å.

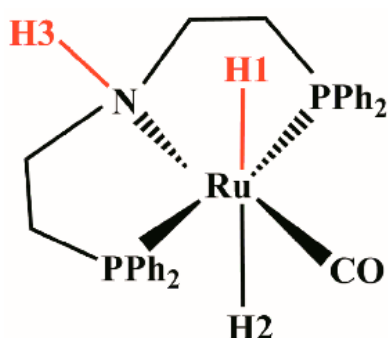
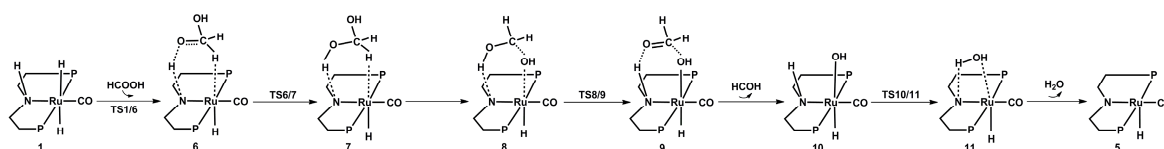


Figure 4. *trans*-RuH<sub>2</sub>(CO)(dpa).

In the beginning, one CO<sub>2</sub> molecule approaches to the hydrogen in catalyst 1, so the Ru-H bond is gradually stretched; thus complex 2 is formed. The bond length of Ru-H is 1.693 Å; the bond angle of CO<sub>2</sub> is 177.8°, which is slightly bended; the formation of complex 2 is 4.6 kcal/mol free energy uphill. Then, the CO<sub>2</sub> molecule in complex 2 takes the hydride from the Ru metal center through the transition state TS2/3 with a 9.3 kcal/mol free energy barrier. Therefore, the formate anion complex 3 is formed with a 4.0 kcal/mol free energy. Next, the complex 4 is formed with a 1.070 Å N-H bond. Complex 4 is 2.8 kcal/mol more uphill than complex 3. Next, a molecular formic acid is released from complex 4. Thus, the unsaturated complex 5 is formed with a 14.2 kcal/mol free energy.

## 2.2. Hydrogenation of Formic Acid

The calculated catalytic process for the reduction of formic acid to formaldehyde and water is shown in Scheme 2. The free energy profile of the second catalytic process is shown in Figure 5. Figure 6 displays the optimized structures of transition states TS1/6, TS6/7, TS8/9, and TS10/11.



Scheme 2. Predicted catalytic process for the hydrogenation of formic acid to formaldehyde and water. Benzene on P atoms are omitted for clarity.

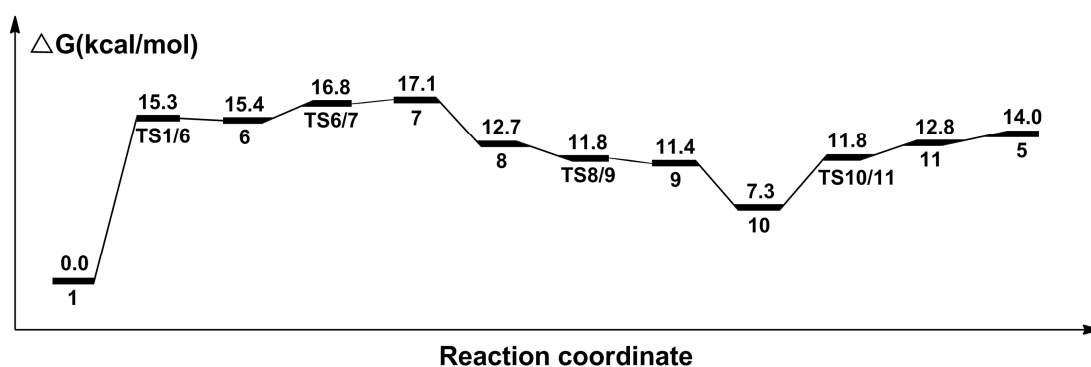
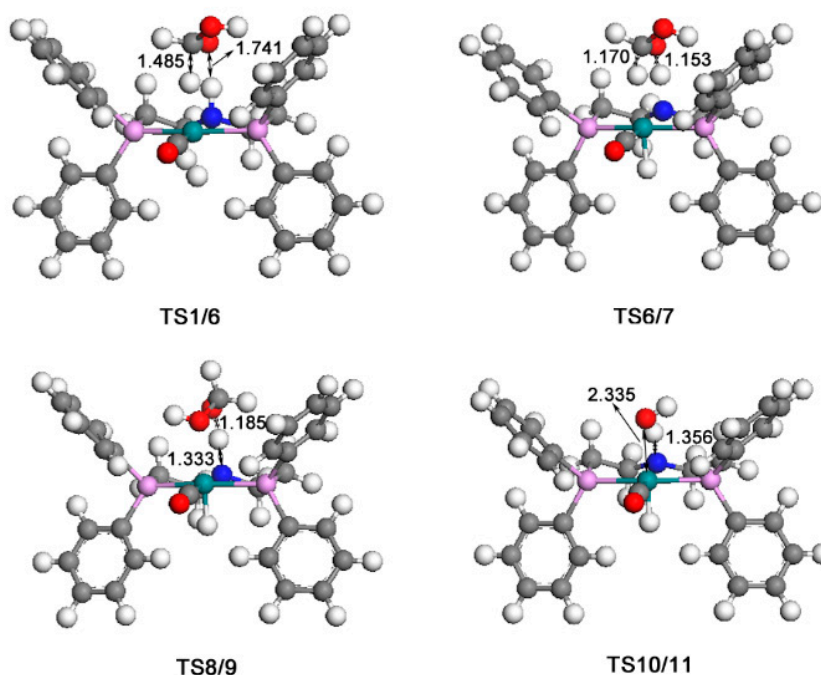


Figure 5. Calculated relative free energies in the catalytic process for the hydrogenation of formic acid to formaldehyde and water.

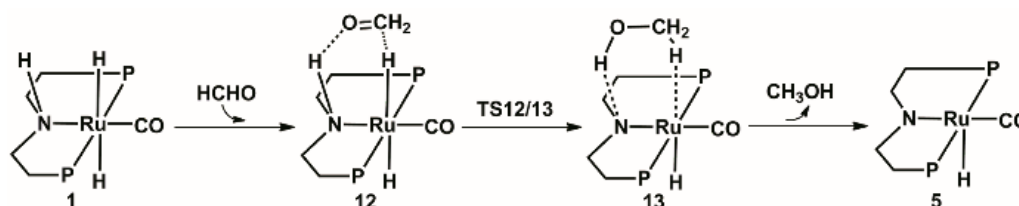
Similarly, in this process, a formic acid molecule firstly approaches catalyst 1; then the formic acid complex **6** is formed through transition state TS1/6 with a free energy barrier of 15.3 kcal/mol. In complex **6**, the Ru-H bond is stretched to 1.858 Å, and the C-H bond is 1.272 Å. Then, complex **7** is formed through a 16.8 kcal/mol transition state TS6/7. In complex **7**, the carbon atom and oxygen atom respectively take the hydride and the proton on the nitrogen side arm of the PNP ligands. Next, the complex **8** is formed with the hydroxyl addition to the Ru center. Then, the nitrogen side arm of the PNP ligands gets the proton through transition state TS8/9. Next, the C-O bond of CH<sub>2</sub>OHO<sup>-</sup> splits, and an 11.4 kcal/mol complex **9** is formed. Then, a formaldehyde molecule is released from complex **9**, so a hydroxyl complex **10** is therefore formed, where the Ru-O bond is 2.173 Å. Complex **11** is formed through an 11.8 kcal/mol transition state TS10/11, with one water molecule formed and released from complex **11**. This process produces the unsaturated complex **5**.



**Figure 6.** Optimized structures of TS1/6(432i cm<sup>-1</sup>), TS6/7(644i cm<sup>-1</sup>), TS8/9 (839i cm<sup>-1</sup>), TS10/11 (1008i cm<sup>-1</sup>). The unit of bond lengths is expressed in angstrom (Å). (Green balls: Ru; pink: P; red: O; blue: N; grey: C; white: H).

### 2.3. Hydrogenation of Formaldehyde

The calculated catalytic process for the reduction of formaldehyde to methanol is shown in Scheme 3. The free energy profile of the third catalytic process is shown in Figure 7. The structures of transition state TS12/13 and key intermediate 13 optimized are displayed in Figure 8.



**Scheme 3.** Predicted catalytic process for the hydrogenation of formaldehyde to methanol. Benzene on P atoms are omitted for clarity.

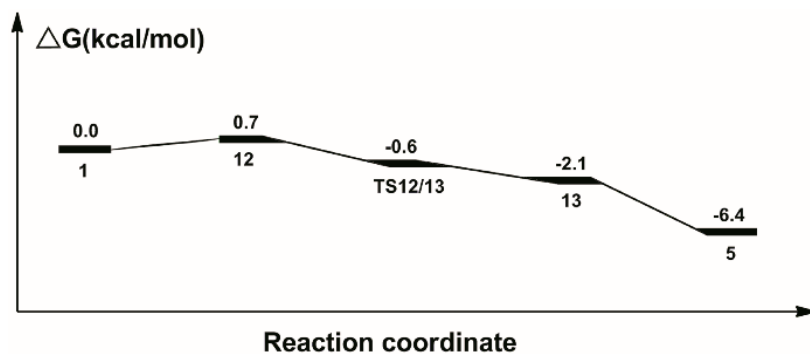


**Figure 7.** Free energy profile for the hydrogenation of formaldehyde to methanol.

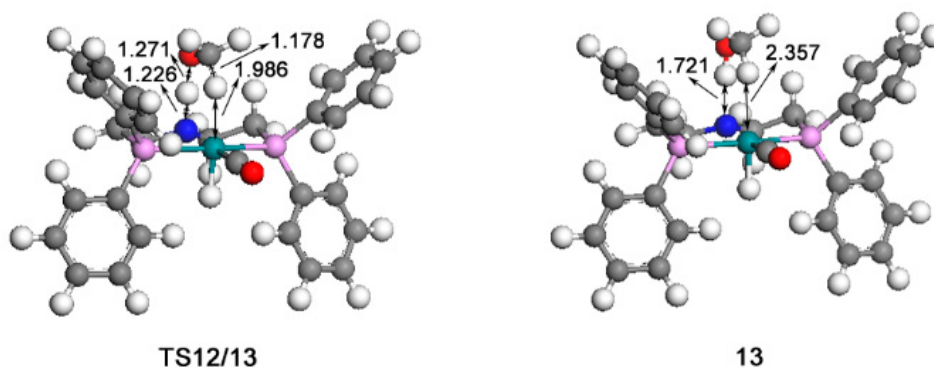


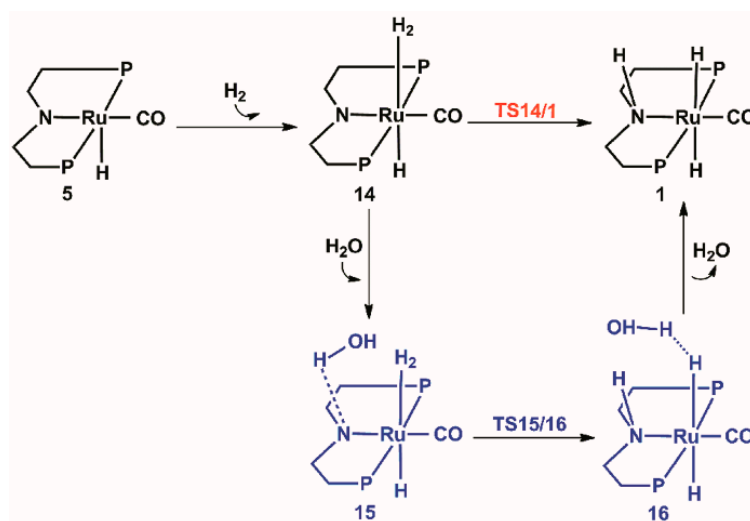
**Figure 8.** Optimized structures of TS12/13 ( $735 \text{ i cm}^{-1}$ ) and 13. The unit of bond lengths is expressed in angstrom ( $\text{\AA}$ ). (Green balls: Ru; pink: P; red: O; blue: N; grey: C; white: H).

Similarly, the unsaturated carbonyl carbon in formaldehyde attacks the hydride on the Ru center. Meanwhile, the oxygen atom in the formaldehyde approaches the proton on the nitrogen side arm of the PNP ligands, to form complex **12**, where the bond length of Ru-H is stretched to  $1.924 \text{ \AA}$ . The bond length of N-H is stretched to  $1.111 \text{ \AA}$ . Next, the hydride and the proton on the nitrogen side arm of the PNP ligands transfers to the formaldehyde for the formation of methanol through transition state TS12/13 with  $0.6 \text{ kcal/mol}$  free energy downhill. Therefore, a methanol molecule is released from the Ru complex **13** and forms an unsaturated complex **5**.

#### 2.4. The Regeneration of the Catalyst

The calculated catalytic process for the regeneration of the catalyst is shown in Scheme 4. The free energy profile of the regeneration of the catalyst is shown in Figure 9. The structures of transition states TS14/1 and TS15/16 optimized are displayed in Figure 10.

Firstly, one  $\text{H}_2$  molecule is added to the vacant position in complex **5**, and thus, a dihydride complex **14** with a  $\text{Ru}\cdots\text{H}_2$  bond of  $1.859 \text{ \AA}$  is formed. The  $\text{H}_2$  cleavage for the regeneration of catalyst **1** can be from two paths: one is the direct cleavage of  $\text{H}_2$  through the transition state TS14/1 ( $14 \text{ U}+2192 \text{ TS14/1}$ ) with a  $21.6 \text{ kcal/mol}$  free energy barrier; the other is that the  $\text{H}_2$  cleavage is assisted by water. So, one molecule of water is added to complex **14**; then, complex **15** is formed, which is lower than complex **14** by  $3.2 \text{ kcal/mol}$ . With the help of water, the N ligands receive protons from water and the dissociative hydroxyl gets the split hydrogen proton through the H-O-H bond for the regeneration of water. Thus, complex **16** is formed through transition state TS15/16 ( $15 \text{ U}+2192 \text{ TS15/16}$ ) with a  $12.7 \text{ kcal/mol}$  free energy barrier. One molecule of water is eventually released from complex **16**, and then the original catalyst is formed.



**Scheme 4.** Predicted catalytic process for the regeneration of the catalyst. Benzene on P atoms are omitted for clarity.

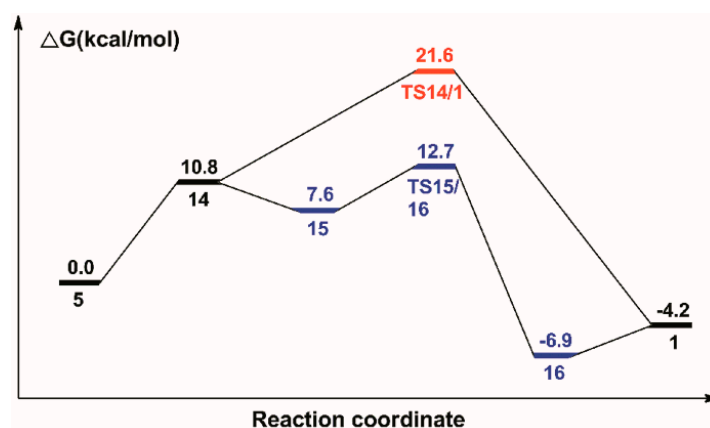


**Figure 9.** Free energy profile for the regeneration of the catalyst.

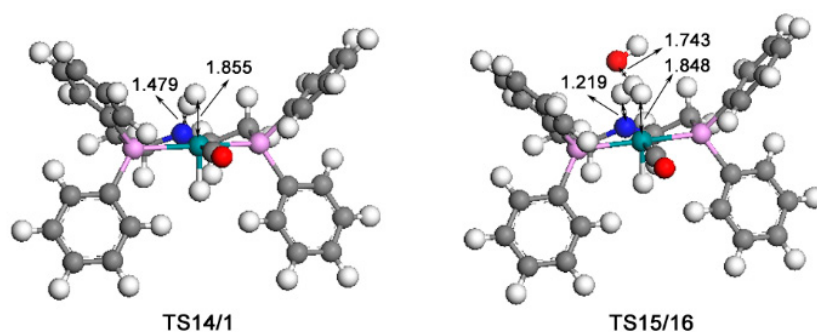


**Figure 10.** Optimized structures of TS14/1 ( $1151\text{ i cm}^{-1}$ ) and TS15/16 ( $806\text{ i cm}^{-1}$ ). The unit of bond lengths is expressed in angstrom ( $\text{\AA}$ ). (Green balls: Ru; pink: P; red: O; blue: N; grey: C; white: H).

### 3. Computational Methods

All the computations achieved were carried out using the Gaussian 09 program [31]. Geometries involved in this work are optimized at the B3LYP level of density functional theory [32,33]. The Stuttgart-Dresden basis set-relativistic effective core potential (RECP) and the Dunning cc-pVDZ basis set [34] are employed respectively for Ru, and P, O, C, N, H atoms for geometry optimizations and

frequency calculations. Considering the solvation effect of tetrahydrofuran (THF), the calculation was performed with the polarizable continuum model (PCM) [35]. Stationary points have been confirmed as minimum or transition states from vibrational frequency calculations. To determine the initial configuration of transition states, we performed potential energy surface (PES) scans. All the transition states calculated were validated using intrinsic reaction coordinate (IRC) calculations. The calculated absolute free energies of all the species and cartesian coordinates for the optimized geometries of all the species are given in Supplementary Materials.

#### 4. Conclusions

In conclusion, the hydrogenation of CO<sub>2</sub> to methanol by the pincer complex *trans*-RuH<sub>2</sub>(CO)(dpa) was investigated by the density functional theory. By computing the cascade catalytic processes, we found that the NH moiety of the ligands is fairly important in the whole catalytic process. In each catalytic process, the NH moiety of the ligands assisted the Ru metal center to complete the catalytic reaction. The results demonstrate that the rate-limiting step in the whole catalytic process is the direct cleavage of H<sub>2</sub> with a free energy barrier of 21.6 kcal/mol. Nevertheless, with water-assist, the free energy can lower to 12.7 kcal/mol. Such a barrier shows that *trans*-RuH<sub>2</sub>(CO)(dpa) is an efficient catalyst for the conversion of CO<sub>2</sub> and H<sub>2</sub> to methanol. The results also provide a foundation for us to design more efficient catalysts. We believe that the new high-efficiency catalysts will be designed using this method.

**Supplementary Materials:** The following are available online at <http://www.mdpi.com/2073-4344/8/6/244/s1>, Table S1: Calculated Gibbs free energies at 298.15 K and 1 atm of all the species, Table S2: Cartesian coordinates for the optimized geometries of all the species.

**Author Contributions:** Methodology, J.L.; Validation, J.L., C.L. and X.L.; Formal Analysis, W.Y.; Data Curation, J.Z.; Writing-Original Draft Preparation, J.Z.; Writing-Review & Editing, L.H.

**Acknowledgments:** This work was supported by the National Natural Science Foundation of China (21476106, 91334202), the Priority Academic Program Development of Jiangsu Higher Education Institutions (PAPD) and Jiangsu Natural Science Foundation (BK20130062, BK2012421). We are grateful to the High Performance Computing Center of Nanjing Tech University for supporting the computational resources. L.L.H. wants to acknowledge the startup support from University of Oklahoma.

**Conflicts of Interest:** The authors declare no conflict of interest.

#### References

1. Jadhav, S.G.; Vaidya, P.D.; Bhanage, B.M.; Joshi, J.B. Catalytic Carbon Dioxide Hydrogenation to Methanol: A Review of Recent Studies. *Chem. Eng. Res. Des.* **2014**, *92*, 2557–2567. [[CrossRef](#)]
2. Nielsen, M.; Alberico, E.; Baumann, W.; Drexler, H.J.; Junge, H.; Gladiali, S.; Beller, M. Low-temperature aqueous-phase methanol dehydrogenation to hydrogen and carbon dioxide. *Nature* **2013**, *495*, 85–89. [[CrossRef](#)] [[PubMed](#)]
3. Alberico, E.; Nielsen, M. Towards a Methanol Economy Based on Homogeneous Catalysis: Methanol to H<sub>2</sub> and CO<sub>2</sub> to Methanol. *Chem. Commun.* **2015**, *51*, 6714–6725. [[CrossRef](#)] [[PubMed](#)]
4. Goeppert, A.; Czaun, M.; Jones, J.P.; Prakash, G.K.S.; Olah, G.A. Recycling of Carbon Dioxide to Methanol and Derived Products-Closing the Loop. *Chem. Soc. Rev.* **2014**, *43*, 7995–8048. [[CrossRef](#)] [[PubMed](#)]
5. Mauna Loa Observatory, Hawaii. Available online: <http://co2now.org/> (accessed on 11 December 2017).
6. Monastersky, R. Global Carbon Dioxide Levels near Worrisome Milestone. *Nature* **2013**, *497*, 13–14. [[CrossRef](#)] [[PubMed](#)]
7. Yang, H.Q.; Xu, Z.H.; Fan, M.H.; Gupta, R.; Slimane, R.B.; Bland, A.E.; Wright, I. Progress in Carbon Dioxide Separation and Capture: A Review. *J. Environ. Sci.* **2008**, *20*, 14–27. [[CrossRef](#)]
8. Yuan, Z.; Eden, M.R.; Gani, R. Toward the Development and Deployment of Large-Scale Carbon Dioxide Capture and Conversion Processes. *Ind. Eng. Chem. Res.* **2016**, *55*, 3383–3419. [[CrossRef](#)]
9. Aresta, M.; Dibenedetto, A.; Angelini, A. Catalysis for the Valorization of Exhaust Carbon: From CO<sub>2</sub> to Chemicals, Materials, and Fuels. Technological Use of CO<sub>2</sub>. *Chem. Rev.* **2014**, *114*, 1709–1742. [[CrossRef](#)] [[PubMed](#)]

10. Aresta, M.; Dibenedetto, A. Utilisation of CO<sub>2</sub> as A Chemical Feedstock: Opportunities and Challenges. *Dalton Trans.* **2007**, *28*, 2975–2992. [[CrossRef](#)] [[PubMed](#)]
11. Centi, G.; Perathoner, S. Opportunities and Prospects in the Chemical Recycling of Carbon Dioxide to Fuels. *Catal. Today* **2009**, *148*, 191–205. [[CrossRef](#)]
12. Wang, W.; Wang, S.; Ma, X.; Gong, J. Recent Advances in Catalytic Hydrogenation of Carbon Dioxide. *Chem. Soc. Rev.* **2011**, *40*, 3703–3727. [[CrossRef](#)] [[PubMed](#)]
13. Porosoff, M.D.; Yan, B.; Chen, J.G. Catalytic Reduction of CO<sub>2</sub> by H<sub>2</sub> for Synthesis of CO, Methanol and Hydrocarbons: Challenges and Opportunities. *Energy Environ. Sci.* **2016**, *9*, 62–73. [[CrossRef](#)]
14. Olah, G.A.; Goepfert, A.; Prakash, G.K.S. Chemical Recycling of Carbon Dioxide to Methanol and Dimethyl Ether: From Greenhouse Gas to Renewable, Environmentally Carbon Neutral Fuels and Synthetic Hydrocarbons. *J. Org. Chem.* **2009**, *74*, 487–498. [[CrossRef](#)] [[PubMed](#)]
15. Moret, S.; Dyson, P.J.; Laurenczy, G. Direct Synthesis of Formic Acid from Carbon Dioxide by Hydrogenation in Acidic Media. *Nat. Commun.* **2014**, *5*, 1–7. [[CrossRef](#)] [[PubMed](#)]
16. Behrens, M.; Studt, F.; Kasatkin, I.; Kuhl, S.; Havecker, M.; Pedersen, F.A.; Zander, S.; Girgsdies, F.; Kurr, P.; Knief, B.L.; et al. The Active Site of Methanol Synthesis over Cu/ZnO/Al<sub>2</sub>O<sub>3</sub> Industrial Catalysts. *Science* **2012**, *336*, 893–897. [[CrossRef](#)] [[PubMed](#)]
17. Li, Y.-N.; Ma, R.; He, L.-N.; Diao, Z.-F. Homogeneous Hydrogenation of Carbon Dioxide to Methanol. *Catal. Sci. Technol.* **2014**, *4*, 1498–1512. [[CrossRef](#)]
18. Cabrera, I.M.; Granados, M.L.; Fierro, J.L.G. Reverse Topotactic Transformation of a Cu-Zn-Al Catalyst during Wet Pd Impregnation: Relevance for the Performance in Methanol Synthesis from CO<sub>2</sub>/H<sub>2</sub> Mixtures. *J. Catal.* **2002**, *210*, 273–284. [[CrossRef](#)]
19. Cabrera, I.M.; Granados, M.L.; Fierro, J.L.G. Pd-Modified Cu-Zn Catalysts for Methanol Synthesis from CO<sub>2</sub>/H<sub>2</sub> Mixtures: Catalytic Structures and Performance. *J. Catal.* **2002**, *210*, 285–294. [[CrossRef](#)]
20. Guo, X.; Mao, D.; Wang, S.; Wu, G.; Lu, G. Combustion Synthesis of CuO-ZnO-ZrO<sub>2</sub> Catalysts for the Hydrogenation of Carbon Dioxide to Methanol. *Catal. Commun.* **2009**, *10*, 1661–1664. [[CrossRef](#)]
21. Grabow, L.C.; Mavrikakis, M. Mechanism of Methanol Synthesis on Cu through CO<sub>2</sub> and CO Hydrogenation. *ACS Catal.* **2011**, *1*, 365–384. [[CrossRef](#)]
22. Bahruji, H.; Bowker, M.; Hutchings, G.; Dimitratos, N.; Wells, P.; Gibson, E.; Jones, W.; Brookes, C.; Morgan, D.; Lalev, G. Pd/ZnO Catalysts for Direct CO<sub>2</sub> Hydrogenation to Methanol. *J. Catal.* **2016**, *343*, 133–146. [[CrossRef](#)]
23. Yang, R.; Yu, X.; Zhang, Y.; Li, W.; Tsubaki, N. A New Method of Low-Temperature Methanol Synthesis on Cu/ZnO/Al<sub>2</sub>O<sub>3</sub> Catalysts from CO/CO<sub>2</sub>/H<sub>2</sub>. *Fuel* **2008**, *87*, 443–450. [[CrossRef](#)]
24. Huff, C.A.; Sanford, M.S. Cascade Catalysis for the Homogeneous Hydrogenation of CO<sub>2</sub> to Methanol. *J. Am. Chem. Soc.* **2011**, *133*, 18122–18125. [[CrossRef](#)] [[PubMed](#)]
25. Wesselbaum, S.; Stein, T.V.; Klankermayer, J.; Leitner, W. Hydrogenation of Carbon Dioxide to Methanol by Using a Homogeneous Ruthenium-Phosphine Catalyst. *Angew. Chem. Int. Ed.* **2012**, *51*, 7499–7502. [[CrossRef](#)] [[PubMed](#)]
26. Haunschild, R. Theoretical study on the reaction mechanism of carbon dioxide reduction to methanol using a homogeneous ruthenium(II) phosphine catalyst. *Polyhedron* **2015**, *85*, 543–548. [[CrossRef](#)]
27. Kuriyama, W.; Matsumoto, T.; Ino, Y.; Ogata, O. Novel Ruthenium Carbonyl Complex Having a Tridentate Ligand and Manufacturing Method and Usage Therefor. PCT International Patent Application WO/2011/048727 A1, 28 April 2011.
28. Kuriyama, W.; Matsumoto, T.; Ogata, O.; Ino, Y.; Aoki, K.; Tanaka, S.; Ishida, K.; Kobayashi, T.; Sayo, N.; Saito, T. Catalytic Hydrogenation of Esters. Development of an Efficient Catalyst and Processes for Synthesising (R)-1,2-Propanediol and 2-(1-Menthoxy)ethanol. *Org. Process Res. Dev.* **2012**, *16*, 166–171. [[CrossRef](#)]
29. Han, Z.; Rong, L.; Wu, J.; Zhang, L.; Wang, Z.; Ding, K. Catalytic Hydrogenation of Cyclic Carbonates: A Practical Approach from CO<sub>2</sub> and Epoxides to Methanol and Diols. *Angew. Chem. Int. Ed.* **2012**, *51*, 13041–13045. [[CrossRef](#)] [[PubMed](#)]
30. Otsuka, T.; Ishii, A.; Dub, P.A.; Ikariya, T. Practical Selective Hydrogenation of  $\alpha$ -Fluorinated Esters with Bifunctional Pincer-Type Ruthenium(II) Catalysts Leading to Fluorinated Alcohols or Fluoral Hemiacetals. *J. Am. Chem. Soc.* **2013**, *135*, 9600–9603. [[CrossRef](#)] [[PubMed](#)]

31. Frisch, M.J.; Trucks, G.W.; Schlegel, H.B.; Scuseria, G.E.; Robb, M.A.; Cheeseman, J.R.; Scalmani, G.; Barone, V.; Mennucci, B.; Petersson, G.A.; et al. *Gaussian 09 (Revision A.02)*; Gaussian, Inc.: Wallingford, CT, USA, 2009.
32. Csonka, G.I.; Ruzsinszky, A.; Tao, J.; Perdew, J.P. Energies of Organic Molecules and Atoms in Density Functional Theory. *Int. J. Quantum Chem.* **2005**, *101*, 506–511. [[CrossRef](#)]
33. Xin, D.; Sader, C.A.; Fischer, U.; Wagner, K.; Jones, P.J.; Xing, M.; Fandrick, K.R.; Gonnella, N.C. Systematic Investigation of DFT-GIAO  $^{15}\text{N}$  NMR Chemical Shift Prediction Using B3LYP/cc-pVDZ: Application to Studies of Regioisomers, Tautomers, Protonation States and N-oxides. *Org. Biomol. Chem.* **2017**, *15*, 928–936. [[CrossRef](#)] [[PubMed](#)]
34. Woon, D.E.; Dunning, T.H. Gaussian Basis Sets for Use in Correlated Molecular Calculations. III. The Atoms Aluminum through Argon. *J. Chem. Phys.* **1993**, *98*, 1358–1371. [[CrossRef](#)]
35. Cossi, M.; Scalmani, G.; Rega, N.; Barone, V. New Developments in the Polarizable Continuum Model for Quantum Mechanical and Classical Calculations on Molecules in Solution. *J. Chem. Phys.* **2002**, *117*, 43–54. [[CrossRef](#)]



© 2018 by the authors. Licensee MDPI, Basel, Switzerland. This article is an open access article distributed under the terms and conditions of the Creative Commons Attribution (CC BY) license (<http://creativecommons.org/licenses/by/4.0/>).